

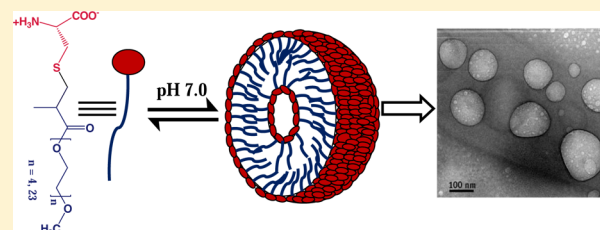
# Vesicle Formation by L-Cysteine-Derived Unconventional Single-Tailed Amphiphiles in Water: A Fluorescence, Microscopy, and Calorimetric Investigation

Rita Ghosh and Joykrishna Dey\*

Department of Chemistry, Indian Institute of Technology, Kharagpur 721 302, India

## Supporting Information

**ABSTRACT:** Two new L-cysteine-derived zwitterionic amphiphiles with poly(ethylene glycol) methyl ether (mPEG) tail of different chain lengths were synthesized and their surface activity and self-assembly properties were investigated. In aqueous phosphate buffered solution of pH 7.0, the amphiphiles were observed to form stable unilamellar vesicles, the bilayer membrane of which is constituted by the mPEG chains. The vesicle phase was characterized by a number of methods including fluorescence spectroscopy, dynamic light scattering, and transmission electron microscopy. The thermodynamics of self-assembly was also studied by isothermal titration calorimetry through measurements of the standard Gibbs free energy change ( $\Delta G_m^\circ$ ), standard enthalpy change ( $\Delta H_m^\circ$ ) and standard entropy change ( $\Delta S_m^\circ$ ) of micellization. The self-assembly process was found to be entropy-driven, which implies that the mPEG chain behaves like a hydrocarbon tail of conventional surfactants. The effects of pH, temperature, salt, and aging time on the bilayer stability were also investigated. Encapsulation and pH-triggered release of model hydrophobic and hydrophilic drugs is demonstrated.



## INTRODUCTION

The vesicles or liposomes (phospholipid-based vesicles) have drawn a great deal of attention due to their widespread application as controlled drug delivery vehicles in the pharmaceutical industry,<sup>1-3</sup> and as model biomembranes in chemistry.<sup>4,5</sup> Lundhal and Yang have utilized liposomes for separating biomolecules.<sup>6</sup> Because vesicles consist of a lipophilic membrane and an interior aqueous reservoir, they can entrap large quantities of substances (hydrophobic or hydrophilic) either in the lipophilic membrane or in the aqueous core making them potential encapsulants of cosmetics in commercial applications. Liposomes have been successfully used for the treatment of cancers, infectious and autoimmune diseases, as well as ocular inflammation.<sup>7-9</sup> There are many reports on vesicle formation from natural surfactants such as phospholipids<sup>10,11</sup> as well as synthetic surfactants.<sup>12,13</sup> Usually, small amphiphilic molecules with a polar hydrophilic headgroup and two long hydrocarbon (either fully saturated or partially unsaturated) tail exhibit vesicle formation in aqueous medium above their critical micelle concentration (*cmc*). However, examples of vesicle formation by single-tailed amphiphilic molecules are not rare.<sup>14,15</sup> Also, there are reports on vesicle formation by a mixture of two single-tailed surfactants with oppositely charged headgroup.<sup>16,17</sup> Synthetic vesicles have gained the most attention not only for providing the fundamental insight on the self-assembly phenomena,<sup>18-20</sup> but also for a myriad of applications in biomedicine, tissue engineering, gene therapy, and drug delivery.<sup>21-25</sup>

Generally, small amphiphilic molecules with a polar hydrophilic headgroup and a long chain hydrocarbon tail exhibit

good surface activity and self-assembling properties in aqueous solution due to the difference in interaction of the two segments of the same molecule with water.<sup>26</sup> However, recently, cationic and anionic surfactants containing poly(ethylene glycol) methyl ether (mPEG) tail that formed self-assembled microstructures were reported from our laboratory.<sup>27,28</sup> In fact, amphiphiles containing PEG chain have become a topic of interest due to their biocompatibility and anomalous behavior in water.<sup>29</sup> It is well-known that PEGs of low molecular weight ( $M_n < 1500$ ) are hydrophilic.<sup>30</sup> The replacement of a  $-\text{CH}_2-$  by oxygen ( $-\text{O}-$ ) along the hydrocarbon,  $-(\text{CH}_2)_n-$ , chain increases its polarity, thereby favoring its interaction with water. Therefore, when PEG chain is covalently linked to another polar headgroup, the resulting molecule is not expected to be surface-active and self-assemble to form aggregates in water. Thus, traditionally, PEGs are coupled to hydrophobic molecules to develop nonionic surfactants.<sup>31,32</sup> Many nonionic surfactants, for example, Tween-20, Triton-X-100, and so forth, in which the PEGs act as the polar headgroup are well-known. On the other hand, micelle-forming copolymers of PEGs with different hydrophobic blocks, such as poly(L-amino acids),<sup>33</sup> diacyllipids,<sup>34</sup> poly(propylene oxide), and so forth, have been used to prepare drug-loaded micelles by direct entrapment of drug into the micellar core, precluding covalent attachment of drug molecules to core-forming blocks. Custers et al. have reported that

Received: June 10, 2014

Revised: September 23, 2014

Published: October 21, 2014

modified Pluronic P85 could be used to allow the thermoreversible binding of multivalent cations in the aqueous shell of micelles. Again, the incorporation of carboxylic acid moieties into PEG-based nonionic surfactants showing a pH-controlled micellar system has been reported by Morikawa and coworker.<sup>35</sup> However, to the best of our knowledge, there are only a couple of reports, one on anionic<sup>27</sup> and the other on cationic<sup>28</sup> surfactant from our group, on the surface activity and self-assembly formation of low-molecular-weight amphiphiles formed by coupling of PEG chain to an ionic headgroup, but there is no report so far on zwitterionic surfactants with PEG as hydrophobic tail. Zwitterionic surfactants are attractive candidates for delivery vehicles of pharmaceutical formulations and also for industrial applications owing to their ability to form different assemblies at different pH. Zwitterionic surfactants having both negative and positive charges in the molecule exhibit pH-dependent behavior and are less irritating to skin and eyes than anionic and cationic surfactants.<sup>36</sup> Additionally, they show better wettability, good biocompatibility, and excellent synergism with other surfactants.<sup>37</sup> These unique properties enable them to find practical use in personal care, household cleaning, and cosmetics.<sup>38</sup>

A number of vesicle-forming amphiphiles consisting of long hydrocarbon tail and amino acid head are reported in the literature,<sup>39,40</sup> but there is no report, so far, on self-assembly formation by amphiphilic molecules consisting of mPEG tail and amino acid head. Therefore, in this work, we have synthesized two zwitterionic amphiphiles mPEG<sub>300</sub>-Cys and mPEG<sub>1100</sub>-Cys (see Figure 1 for structures) bearing mPEG tail

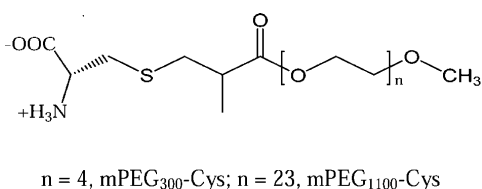


**Figure 1.** Molecular structures of mPEG<sub>300</sub>-Cys and mPEG<sub>1100</sub>-Cys.

of different chain lengths and L-cysteine as the polar headgroup. It was intended to examine if there is any micellization by this new class of amphiphiles when the ionic head is replaced by a charged neutral zwitterionic headgroup. Zwitterionic surfactants with mPEG tail are advantageous because the amphiphiles are pH-sensitive. Also, since both mPEGs and L-cysteine are biocompatible and eco-friendly, their self-assembled structures in aqueous medium can have potential applications in drug delivery. Moreover, these amphiphiles are very easy to synthesize. Therefore, aggregation behavior of these amphiphiles was thoroughly investigated in pH 7.0 buffer at 25 °C. Interfacial properties of the amphiphiles were studied by the surface tension method. The *cmc* values, micropolarity, and microviscosity of the aggregates were measured by the fluorescence probe technique. The thermodynamics of the self-assembly process was investigated by isothermal titration calorimetry through measurements of the standard free energy change ( $\Delta G_m^\circ$ ), standard enthalpy change ( $\Delta H_m^\circ$ ), and standard entropy change ( $\Delta S_m^\circ$ ) of micellization. Dynamic light scattering was used to determine the hydrodynamic diameters of the aggregates. The shape of the aggregates was investigated by use of transmission electron microscopy. The stability of the aggregates with respect to concentration, solution pH, temperature, and aging time was studied.

Encapsulation and pH-triggered release of model hydrophobic and hydrophilic drugs will also be demonstrated.

## EXPERIMENTAL SECTION

**Materials.** Fluorescence probes, *N*-phenyl-1-naphthylamine (NPN), pyrene (Py), coumarin-153 (C153), and 1,6-diphenyl-1,3,5-hexatriene (DPH) were purchased from Sigma-Aldrich (Bangalore, India) and were recrystallized from acetone–ethanol mixture at least twice before use. Purity of the probes was confirmed by the fluorescence excitation spectra. Poly(ethylene glycol) methyl ether methacrylate (mPEG; MW 300 and 1100) were obtained from Sigma-Aldrich. L-Cysteine was procured from Lab Chem and used without further purification. Analytical grade sodium dihydrogen phosphate ( $\text{NaH}_2\text{PO}_4$ ) and disodium monohydrogen phosphate ( $\text{Na}_2\text{HPO}_4$ ) were purchased from SRL, Mumbai. Super dry methanol and super dry triethylamine (TEA) were used for synthesis. Milli-Q water (18 M $\Omega$ ) was used for the aqueous solution preparation.

The amphiphiles were synthesized by the Michael addition reaction of L-cysteine with poly(ethylene glycol) methyl ether methacrylate by thiol–ene “click” chemistry according to the method reported by our group.<sup>41</sup> The details of the chemical identifications like FT-IR spectra, <sup>1</sup>H and <sup>13</sup>C NMR and the synthetic scheme have been presented in the Supporting Information (SI).

## METHODS AND INSTRUMENTATION

The <sup>1</sup>H and <sup>13</sup>C NMR spectra were recorded on a Bruker SEM 200 instrument using tetramethyl silane (TMS) as the internal standard. Melting points were determined with an InstInd (Kolkata) melting point apparatus in open capillaries. The pH measurements were done with digital pH meter (Model 111, India) using a glass electrode. A PerkinElmer model 883 IR spectrometer was used for recording FT-IR spectra. The measurements of optical rotations were performed on a Jasco P-1020 digital polarimeter. Turbidity ( $\tau$ ) measurements were performed on a Shimadzu 1601 (Japan) UV-vis spectrophotometer at 400 nm using a quartz cell with a path length of 1 cm. All measurements were carried out at 25 °C unless otherwise mentioned.

Surface tension ( $\gamma$ ) measurements were performed on a GBX 3S (France) surface tensiometer using the Du Nüoy ring method. The steady-state fluorescence measurements were performed either on a PerkinElmer LS-55 luminescence spectrometer equipped with a temperature-controlled cell holder or on a Horiba FL3-11 spectrophotometer. Again, a SPEX Fluorolog-3 (model no. FL3-11) spectrophotometer was used for recording fluorescence emission spectra of Py. Optical Building Blocks Corporation EasyLife instrument was employed to measure the fluorescence lifetime of the DPH probe. The dynamic light scattering (DLS) measurements were performed with Zetasizer Nano ZS (Malvern Instrument Lab, Malvern, U.K.) light scattering spectrometer equipped with a He–Ne laser operated at 4 mW ( $\lambda_0 = 632.8$  nm) at 25 °C. The same instrument was used to measure surface zeta ( $\zeta$ ) potential of the vesicles. The morphology of the aggregates was investigated by a transmission electron microscope (FEI-TECNAI G2 20S-TWIN, FEI, USA) operating at an accelerating voltage of 80 kV. A microcalorimeter of Microcal iTC<sub>200</sub> (made in U.S.A) was used for thermometric measurements. The details of surface tension, fluorescence, isothermal titration calorimetry (ITC), transmission electron microscopy (TEM), and DLS are described in the SI.

## RESULTS AND DISCUSSION

**Interfacial Properties.** To understand the surface activity, we have performed surface tension measurements for mPEG<sub>300</sub>-Cys and mPEG<sub>1100</sub>-Cys in phosphate buffer at pH 7.0. As shown by the plots of surface tension ( $\gamma/\text{mN m}^{-1}$ ) versus surfactant concentration ( $\log C_s$ ) in Figure S1 (SI), the  $\gamma$ -value decreases gradually with the increase of  $C_s$ , suggesting spontaneous adsorption of the surfactants at the air/water interface. However, the adsorption efficiency,  $pC_{20}$  ( $= -\log C_{20}$ ,

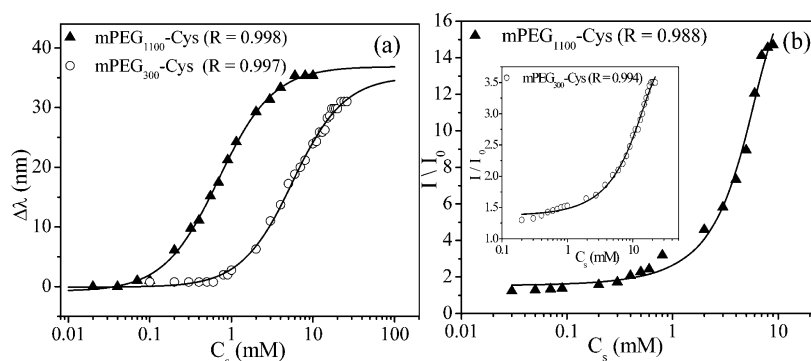


**Figure 2.** Plots of (a) spectral shift ( $\Delta\lambda$ ) and (b) relative fluorescence intensity ( $I/I_0$ ) of NPN as a function of  $C_s$  in pH 7.0 at 25 °C; mPEG<sub>300</sub>-Cys (○), mPEG<sub>1100</sub>-Cys (▲).

**Table 1.** Critical Micelle Concentration ( $cmc$ ), Standard Gibbs Free Energy Change ( $\Delta G_m^\circ$ ), Standard Enthalpy Change ( $\Delta H_m^\circ$ ), and Standard Entropy Change ( $\Delta S_m^\circ$ ) of the Vesicle Formation in Aqueous Buffered Solution (pH 7.0) by mPEG<sub>300</sub>-Cys and mPEG<sub>1100</sub>-Cys at 25 °C

surfactant	$cmc$ (mM)		$\Delta G_m^\circ$ (kJ mol <sup>-1</sup> )	$\Delta H_m^\circ$ (kJ mol <sup>-1</sup> )	$\Delta S_m^\circ$ (J K <sup>-1</sup> mol <sup>-1</sup> )	$T\Delta S_m^\circ$ (kJ mol <sup>-1</sup> )
	fluorescence (NPN)	ITC				
mPEG <sub>300</sub> -Cys	1.0 (± 0.07)	1.13 (± 0.02)	-16.81	0.42 (± 0.1)	57.82	17.23
mPEG <sub>1100</sub> -Cys	0.2 (± 0.03)	0.15 (± 0.03)	-21.81	2.20 (± 0.15)	80.57	24.01

where  $C_{20}$  is the molar concentration of the surfactant required to reduce  $\gamma$  by 20 units) is less for both mPEG<sub>300</sub>-Cys (2.28) and mPEG<sub>1100</sub>-Cys (2.36). The reduction of  $\gamma$ -value is much less in comparison to conventional hydrocarbon chain surfactants.<sup>39,40</sup> This can be attributed to the hydrophilic nature of the mPEG chain in comparison to hydrocarbon tail. Interestingly, unlike conventional surfactants, none of the plots show any break followed by a plateau in the investigated concentration range. This is because in aqueous medium, depending upon the pH, both mPEG<sub>300</sub>-Cys and mPEG<sub>1100</sub>-Cys are expected to be present in the zwitterionic, cationic, or anionic forms. The  $pK_a$  values of the cation–zwitterion and zwitterion–anion equilibria obtained from fluorescence probe studies discussed below are, respectively, 3.9 and 9.3 for mPEG<sub>300</sub>-Cys and 5.1 and 9.1 for mPEG<sub>1100</sub>-Cys. The pI values thus obtained are 6.6 for mPEG<sub>300</sub>-Cys and 7.1 for mPEG<sub>1100</sub>-Cys. This means that, in pH 7 phosphate buffer, the amphiphiles should be present mainly in the zwitterionic form. Further, the mPEG chain is known to be polar. As a result, the polarity difference between the mPEG tail and zwitterionic amino acid headgroup is small compared to that of hydrocarbon chain containing conventional surfactants. For this reason, the mPEG containing zwitterionic amphiphiles behave like long chain fatty alcohols in water. The surface behavior of the fatty alcohols in water has been discussed elaborately by Posner et al.<sup>42</sup>

**Fluorescence Probe Studies.** Fluorescence study by using different extrinsic probe molecules has been proven to be a useful technique to probe into the microenvironment of the aggregates and also to evaluate the  $cmc$  value of surfactant in aqueous solution.<sup>43</sup> In this study, NPN, C153, Py, and DPH were used as efficient extrinsic probes to investigate the microenvironment of the self-assemblies. These probes are nonpolar molecules and they preferentially get solubilized in the hydrophobic microdomain of the surfactant aggregates. The fluorescence spectra of these probes are sensitive to the

environment around them and, thus, can provide insight into the surfactant self-assemblies and microstructure formation.

**Fluorescence Titration with NPN Probe.** NPN has been extensively used as an efficient fluorescence probe as it exhibits a large spectral shift along with a huge intensity enhancement upon incorporation into the hydrophobic microdomain of the aggregates.<sup>44</sup> In the present study, the self-assembling properties of mPEG<sub>300</sub>-Cys and mPEG<sub>1100</sub>-Cys were investigated by NPN in pH 7.0 at 25 °C. In the presence of the surfactants, the emission maximum of NPN exhibits a 30–35 nm blue shift accompanied by a huge enhancement of emission intensity relative to that in pH 7.0 buffer (Figure S2, SI). The large blue shift of the emission maximum of NPN suggests its encapsulation within nonpolar environment of the aggregates formed by the surfactants in aqueous buffered solution. In addition, the enhancement of the fluorescence intensity indicates that the microenvironment of NPN probe is viscous. The variations of the spectral shift of wavelength  $\Delta\lambda$  [ $\Delta\lambda = \lambda_{\max}(\text{water}) - \lambda_{\max}(\text{surfactant})$ ] of emission maximum and relative fluorescence intensity,  $I/I_0$  (where  $I_0$  and  $I$  are the fluorescence intensities at  $\lambda = 430$  nm in pure buffer and in the presence of surfactant, respectively) of NPN probe with surfactant concentration ( $C_s$ ) are depicted in Figure 2. The sigmoid plot corresponding to a two-state transition clearly suggests the existence of equilibrium between surfactant monomers and aggregates. The  $cmc$  values (Table 1) obtained from the onset of the rise of the curves (Figure 2a) are 1.0 mM and 0.2 mM for mPEG<sub>300</sub>-Cys and mPEG<sub>1100</sub>-Cys, respectively. It can be mentioned here that due to the presence of longer mPEG chain of mPEG<sub>1100</sub>-Cys, the  $cmc$  value of mPEG<sub>1100</sub>-Cys is less than that of mPEG<sub>300</sub>-Cys.<sup>27</sup> Thus, it can be concluded that the amphiphiles with mPEG chain behave like conventional hydrocarbon tail surfactants.

**Micropolarity of the Self-Assemblies. Study with C153 Probe.** C153 has been employed as a polarity probe as well as a solvation dynamics probe in a number of studies.<sup>45</sup> Thus, the

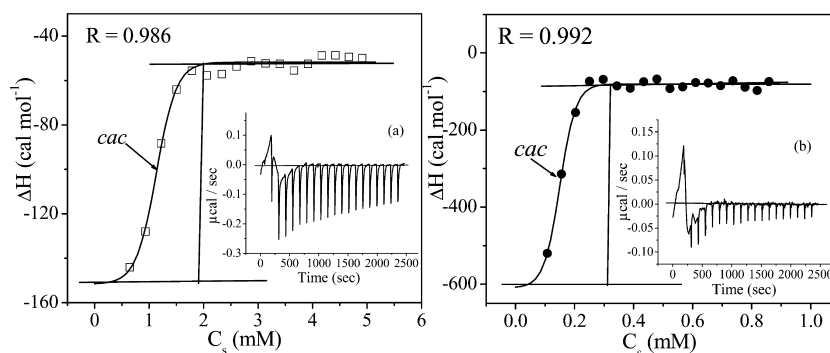


**Figure 3.** Plots of variation of change in enthalpy ( $\Delta H$ ) versus  $C_s$  at 25 °C: (□) mPEG<sub>300</sub>-Cys and (●) mPEG<sub>1100</sub>-Cys. Inset: thermogram of the respective titration.

microenvironment formed by the mPEG chains was investigated by C153 probe molecule. C153 is relatively more polar than NPN. Therefore, the variation of  $\Delta\lambda$  with the increase in  $C_s$  (Figure S3, SI) is small compared to that obtained in NPN probe study. The fluorescence emission spectra of C153 measured in pH 7.0 buffer in the absence and in the presence of different  $C_s$  are depicted in Figure S4 of the SI. In addition to providing information regarding aggregate formation, C153 can also correlate the microenvironment of the self-assembly with solvents of different polarity with the help of characteristic steady-state emission spectrum.<sup>46</sup> Micropolarity of the self-assemblies can thus be evaluated by the emission frequency of C153 ( $\bar{\nu}_{em}$ ). Micropolarity is expressed in terms of solvent polarity scale ( $\pi^*$ ). The relationship between  $\bar{\nu}_{em}$  and  $\pi^*$  is given by eq 1. The  $\pi^*$  values obtained were 0.74 for mPEG<sub>300</sub>-Cys and 0.62 for mPEG<sub>1100</sub>-Cys, which suggest that the polarities of the microenvironments of C153 probe were comparable to those of propionaldehyde ( $\pi^* = 0.71$ ) and acetone ( $\pi^* = 0.62$ ), respectively.<sup>46</sup>

$$\bar{\nu}_{em} = 21.217 - 3.505\pi^* \quad (1)$$

**Study with Py Probe.** The microenvironment of the self-assemblies was also investigated by Py molecule, particularly to evaluate the micropolarity of the aggregates. The solvent dependence of vibronic band intensities in Py fluorescence has captured great attention in the literature. The intensities of the various vibronic bands were found to depend strongly on the solvent polarity.<sup>47</sup> More specifically, the ratio ( $I_1/I_3$ ) of the intensities of the first ( $I_1$ , 372 nm) to the third ( $I_3$ , 384 nm) vibronic bands in the fluorescence spectrum of Py is very sensitive to solvent polarity change.<sup>48</sup> Therefore, the  $I_1/I_3$  ratio is referred to as micropolarity index. The polarity ratios for different organic solvents are reported by Kalyansundaram et al.<sup>47</sup> So, the  $I_1/I_3$  ratio was measured in the presence and absence of different surfactant concentrations (Figure S5, SI). The  $I_1/I_3$  ratio has a value of 1.75 in pH 7.0 in the absence of the surfactant, but the ratio falls off with increasing concentration of the added surfactant, indicating the formation of aggregates with less polar local environment. The minimum values of  $I_1/I_3$  were found to be 1.54 (mPEG<sub>300</sub>-Cys) and 1.46 (mPEG<sub>1100</sub>-Cys), which correspond to the dielectric constant of *N*-methyl formamide ( $I_1/I_3 = 1.56$ ) and acetone ( $I_1/I_3 = 1.46$ ), respectively.<sup>47</sup> This reveals that the microenvironments formed by the surfactants with mPEG chain are hydrophilic relative to that for common long chain hydrocarbon surfactants.<sup>39,40</sup> Thus, the micropolarity of the self-assemblies evaluated from both of

the above probe studies (C153 and Py) show a good degree of agreement with each other.

**Microviscosity of the Self-Assemblies.** The steady-state fluorescence anisotropy ( $r$ ) measurement was carried out with the help of DPH probe to further investigate the microenvironment formed by the mPEG chains. DPH is a well-known membrane fluidity probe and its  $r$ -value can be used as an index of membrane rigidity of liposomes or vesicles.<sup>49,50</sup> The  $r$ -values were found to be 0.168 and 0.183 for mPEG<sub>300</sub>-Cys (5 mM) and mPEG<sub>1100</sub>-Cys (2 mM), respectively. Such high  $r$ -values imply tight packing of mPEG chains housing the DPH probe, which is indicative of bilayer formation.<sup>49</sup> The concentration-dependent anisotropy study was also carried out to measure the variation of microfluidity at different concentrations. SI Figure S6 clearly suggests that with the increase in surfactant concentration, the  $r$ -value increases up to a particular concentration and then becomes constant, which suggests formation of a more rigid microenvironment with increase in surfactant concentration.

The rigidity of the microenvironment of the self-assemblies is also manifested by the large microviscosity ( $\eta_m$ ) values, calculated from the Debye-Stokes-Einstein relation<sup>51</sup> using the steady-state fluorescence anisotropy ( $r$ ) and fluorescence lifetime ( $\tau_f$ ) data of DPH probe (SI Table S1). It is also reported that the  $\tau_f$  value of DPH in nonpolar and viscous solvents is usually observed to be greater than 4 ns.<sup>52</sup> Therefore, time-resolved fluorescence measurement by using DPH probe in the presence of 15 mM mPEG<sub>300</sub>-Cys and 5 mM mPEG<sub>1100</sub>-Cys was carried out to examine the lifetime of the probe molecule in the hydrophobic microdomain of the self-assemblies and also to evaluate the microviscosity of the aggregates. The experimental time-resolved intensity profile fits well to biexponential decay with  $\chi^2$  values (0.8–1.2) in a fairly accepted range for both the surfactants. The  $\eta_m$  values thus obtained are 65 mPa s and 79 mPa s for mPEG<sub>300</sub>-Cys and mPEG<sub>1100</sub>-Cys, respectively. The  $\eta_m$  values are larger than those of micelle-forming hydrocarbon surfactants such as SDS, DTAB, and CTAB.<sup>50</sup> The large  $\eta_m$  values for both the surfactants suggest bilayer formation at concentration above *cmc*. On the other hand, the low micropolarity index ( $I_1/I_3$ ) and larger spectral shift of NPN probe imply formation of aggregates having a microenvironment less polar compared to water. The 10- to 20-fold increase in fluorescence intensity of NPN probe upon incorporation into the hydrophobic microenvironment is a strong proof of stable and well-packed aggregate formation.

**Thermodynamics of Self-Assembly Formation.** The self-organization (vesicle formation) of surfactants in solution is an important and amply studied thermodynamically favorable physicochemical phenomenon.<sup>53</sup> Although there are a number of methods to determine *cmc* and energetics of the micellization, the thermometric titration method has a distinction in that it can estimate both *cmc* and energetics of surfactant self-organization from a stepwise addition mode, providing an excellent process to evaluate all the thermodynamic parameters in a single run. Generally, thermodynamic parameters are calculated to conjecture the mechanism of self-assembly formation. In the present study, the thermodynamic parameters were determined by ITC for both mPEG<sub>300</sub>-Cys and mPEG<sub>1100</sub>-Cys at 25 °C using different stock concentrations. However, measurements using lower surfactant stock concentration (5 mM of mPEG<sub>300</sub>-Cys and 2 mM of mPEG<sub>1100</sub>-Cys) failed to give reproducible results (see Figure S7, SI). The thermograms obtained by using higher surfactant stock concentration (30 mM of mPEG<sub>300</sub>-Cys and 5 mM of mPEG<sub>1100</sub>-Cys) are presented as insets of Figure 3a,b. The plots show a sigmoid increase of enthalpy with the increase of *C<sub>s</sub>*. The thermodynamic parameters obtained from the plots are included in Table 1. The *cmc* values of mPEG<sub>300</sub>-Cys (~1.1 mM) and mPEG<sub>1100</sub>-Cys (~0.2 mM) were obtained from the inflection point of the respective plot. The *cmc* values thus obtained are close to the corresponding value obtained by fluorometric titration and they correspond to the respective zwitterionic form of the amphiphiles. The  $\Delta H_m^\circ$  value was obtained by subtracting the initial enthalpy from the final enthalpy indicated by the vertical arrow in each figure. Basically, enthalpy levels between nonmicellar and micellar regions give a measure of the enthalpy of micellization.<sup>54</sup> For both the amphiphiles, the vesicle formation procedure is endothermic, which is emphasized by the positive  $\Delta H_m^\circ$  values. The  $\Delta G_m^\circ$  value was calculated from the measured *cmc* value using the following relation:<sup>55</sup>

$$\Delta G_m^\circ = (1 + f)RT \ln cmc \quad (2)$$

where *f* stands for the fraction of counterions bound to a micelle. In this case *f* = 0, as the surfactants are zwitterionic. The  $\Delta S_m^\circ$  was evaluated by the Gibbs equation

$$\Delta S_m^\circ = (\Delta H_m^\circ - \Delta G_m^\circ)/T \quad (3)$$

The spontaneity of vesicle formation is expressed from the very large negative values of  $\Delta G_m^\circ$  and the very large positive values of  $\Delta S_m^\circ$ . Thus,  $T\Delta S_m^\circ$  values for both surfactants are found to be much larger than that of the  $\Delta H_m^\circ$  values, which clearly suggests that the spontaneous aggregate formation is an entropy-driven process. The essence of the entropy-driven process is the hydrophobic interaction.<sup>56</sup> The release of water molecules around the mPEG tails contributes to the entropy rise which is beneficial for the self-assembly process. This means that the aggregation process of mPEG<sub>300</sub>-Cys and mPEG<sub>1100</sub>-Cys is similar to that of most hydrocarbon surfactants. In other words, the mPEG chains behave like hydrocarbon tails.

**Light Scattering Study.** DLS measurements were performed to obtain the mean hydrodynamic size and size distribution of the self-assemblies in pH 7.0 at 25 °C. The size distribution (expressed in percentage volume) profiles for both amphiphiles of different concentrations are depicted in Figure 4. A bimodal distribution is observed, suggesting the coexistence of larger aggregates along with smaller ones.

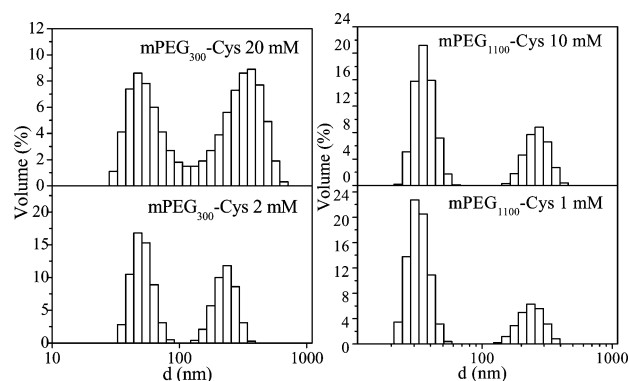


**Figure 4.** Size distribution profiles of mPEG<sub>300</sub>-Cys (2 mM and 20 mM) and mPEG<sub>1100</sub>-Cys (1 mM and 10 mM) in pH 7.0 at 25 °C after 2 h of sample preparation.

Aggregates of two different sizes with mean diameter of about 20–80 nm and 200–500 nm coexist in concentrated as well as in dilute aqueous solutions of the surfactants. From the plots it is also obvious that the mean hydrodynamic diameters remain almost invariant with concentration of the surfactant, indicating stability of the vesicles with respect to concentration dependent phase change.

**Transmission Electron Microscopy.** To further visualize the actual morphology of the aggregates TEM images were taken. Representative TEM images of stained specimens prepared from both surfactant solutions at pH 7.0 buffer are shown in Figure 5a,d. The micrographs clearly reveal the formation of small unilamellar closed vesicles (SUVs) with an aqueous cavity. Close insight into the size and shape of the microstructures shows that the vesicles have distorted spherical shapes of relatively small size (50–200 nm) along with some larger ones. The TEM images (Figure S8, SI) of concentrated surfactant solutions also exhibit large unilamellar vesicles (LUVs). The existence of LUVs at higher concentrations as also indicated by the DLS data (Figure 4) may be attributed to the fusion of the SUVs in the presence of the electric field, produced by the highly energetic electron beam, which again is strong proof of the hydrophobic nature of the PEGs. Thus, the TEM microstructures are consistent with the findings from DLS and fluorescence studies.

**Stability of the Vesicles.** It is well-known that the spontaneously formed surfactant self-assemblies are usually a reversible organization of molecules to a higher-ordered structure and their physical stability can be altered by external stimuli.<sup>40</sup> The vesicle stability was therefore investigated under various physical conditions including time, temperature, pH, salt, and surface charge, emphasizing the stability of spontaneously formed vesicles and their ability in incorporation and exemption of drugs.

**Thermal Stability of the Vesicles.** Temperature is an important factor in self-assembly, and it also affects the size and shape of the aggregate. Fluorescence anisotropy of the DPH probe has been used to observe the phase transitions of the membrane. The effect of temperature on *r*-values was studied using 15 mM mPEG<sub>300</sub>-Cys and 5 mM mPEG<sub>1100</sub>-Cys in pH 7.0. Figure 6 depicts the variation of *r* as a function of temperature. As seen from the plots, *r*-value decreases with the increase in temperature, but it lies in the vesicular range, even at 75 °C. This suggests that the PEG chains become more fluid at elevated temperatures. This is due to weakening of the hydrophobic interactions caused by the thermal motion

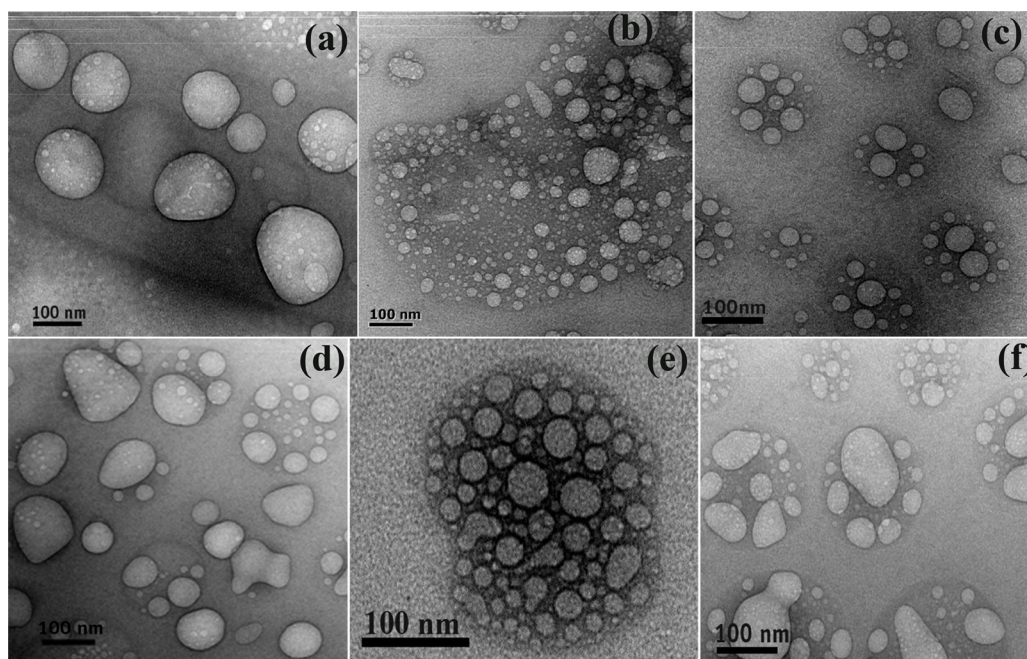


**Figure 5.** Negatively stained (1% uranyl acetate) TEM pictures of 20 mM mPEG<sub>300</sub>-Cys solutions of pH (a) 7.0, (b) 3.0, and (c) 12.0, and 5 mM mPEG<sub>1100</sub>-Cys solutions of pH (d) 7.0, (e) 3.0, and (f) 12.0.

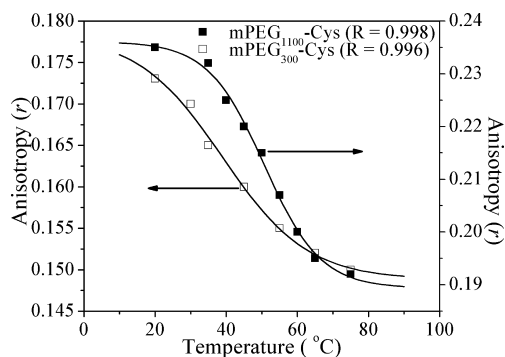


**Figure 6.** Plots showing variation of fluorescence anisotropy ( $r$ ) of DPH with temperature.

among PEG chains. In other words, phase transition from a highly ordered gel-like bilayer state to a slightly less ordered liquid-crystalline state occurs upon increase in temperature. The temperature corresponding to the inflection points of the curves was taken as the melting or phase transition temperature,  $T_m$ , of the bilayer membrane. The high melting temperatures, 52 °C and 43 °C for mPEG<sub>1100</sub>-Cys and mPEG<sub>300</sub>-Cys, respectively, clearly suggest that the vesicles are quite stable at physiological temperature (37 °C). The existence of unilamellar vesicles at higher temperatures (75 °C) is evidenced by the size distribution histogram and TEM picture (Figure S9, SI) of 15 mM mPEG<sub>300</sub>-Cys solution, as a representative example.

**Vesicle Stability with Respect to pH Change.** The pH-sensitive vesicles have shown potential importance in controlled drug release, as the pH around any damaged tissue differs from that of normal tissue. The variation of solution pH shows a predominant change in the bilayer structure and affects the stability of vesicles formed by surfactants with ionizable headgroups. Since the surfactants under study are zwitterionic at neutral pH, the stability of the vesicles was studied by varying

pH of the medium. The pH-stability measurement was carried out by monitoring the fluorescence anisotropy of the DPH probe. The pH of the solution containing fixed concentrations of mPEG<sub>300</sub>-Cys (20 mM) and mPEG<sub>1100</sub>-Cys (5 mM) was varied from 2 to 12 at 25 °C. Each solution was incubated for 30 min prior to the measurement. Figure 7 shows the variation

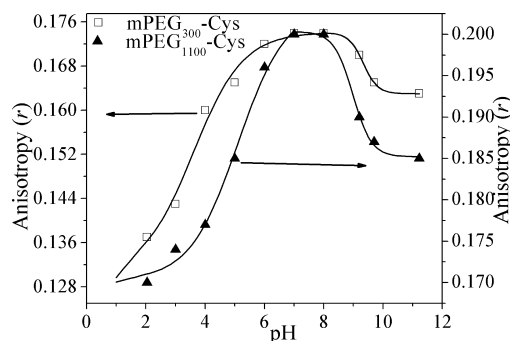
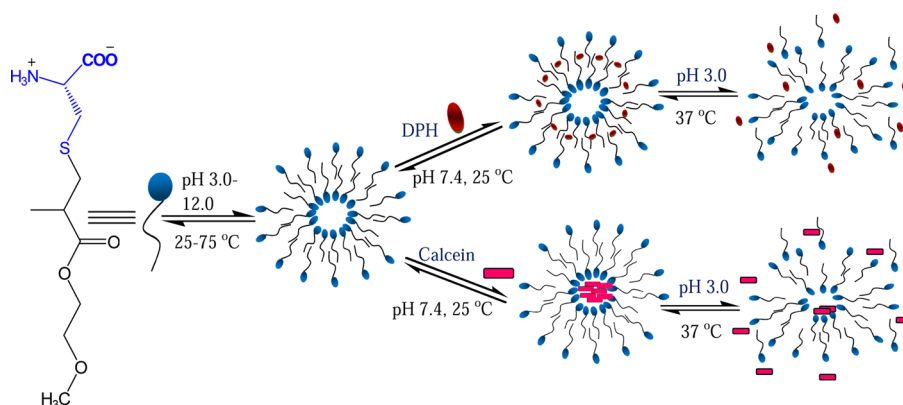


**Figure 7.** Plots of variation of fluorescence anisotropy ( $r$ ) of DPH as a function of pH at 25 °C.

of  $r$ -values with the change in pH of the surfactant solution. It has been found that the  $r$ -values decrease with the decrease in solution pH and show maximum stability at pH ~ 6.5–8. This indicates that the bilayer membranes of vesicular aggregates become less rigid at lower and higher pHs as a result of weakening of the packing of the mPEG units. The weak packing of the mPEG units results from greater electrostatic repulsion between anionic or cationic head groups of the amphiphiles in water than that of the zwitterionic forms. However, in both lower and higher pHs, the  $r$ -values lie in the vesicular range, suggesting the existence of cationic and anionic vesicles, respectively. The  $pK_a$  values for the proton transfer equilibria were evaluated from the pH variation profiles and were found to be 3.9 and 9.3 for mPEG<sub>300</sub>-Cys, and 5.1 and 9.1 for mPEG<sub>1100</sub>-Cys. The  $pI$  values calculated from the respective

**Scheme 1. Schematic Representation of Encapsulation and Release of Dye Molecules (DPH and CAL) at pH 7.4 and Their Release at pH 3.0**



$pK_a$ s are 6.6 and 7.1 for mPEG<sub>300</sub>-Cys and mPEG<sub>1100</sub>-Cys, respectively. This clearly indicates that at pH 7.0 both surfactants remain in the zwitterionic form as shown in Figure 1.

The size distributions (SI Figure S10) of the vesicles in acidic and basic pH solutions of the surfactants were also measured in order to examine if there is any structural change of the vesicles. The hydrodynamic diameters of the species formed in acidic (pH 3) and basic (pH 12) pHs though smaller than that of the corresponding zwitterionic vesicles (see Figure 4), but they are much larger than normal micelles which have diameters in the range of 3–5 nm.<sup>57</sup> The existence of unilamellar vesicles in acidic as well as in basic pH is further confirmed by the respective TEM picture in Figure 5.

**Aging Effect.** Vesicle stability was also confirmed with respect to time. The turbidity ( $\tau$ ) of the surfactant solutions was measured over a period of one month taking 6 mM mPEG<sub>300</sub>-Cys and 2.5 mM mPEG<sub>1100</sub>-Cys in pH 7.0 buffer at 400 nm to ensure vesicle stability. The turbidity of a colloidal solution is mainly caused by the scattering of light by the vesicular aggregates, and the extent of turbidity depends on the size and population of vesicles. Figure S11 (see SI) shows a slight increase in turbidity for both surfactant solutions in the initial aging interval, which remains constant thereafter at the equilibrium value ( $\sim 30\%$ ) for about 30 days. The formation and growth of the vesicles cause the initial increase of turbidity while the subsequent constant turbidity indicates evolution of high stability with aging time, which is also supported by the size distribution profiles (Figure S12, SI). Thus, for both systems, the vesicles are found to be fairly stable. It should be noted here that the vesicular solutions of both surfactants at pH 3.0 and 12.0 did not show any change of turbidity after storage for a month. This is expected as the vesicles in these solutions are ionic in character; they repel each other, thus preventing any intervesicular interaction that enlarges the vesicle.

On the other hand, the vesicles in neutral pH are relatively less stable because the overall electric charge of the vesicles is zero, as indicated by the zeta ( $\zeta$ ) potential value. The  $\zeta$ -potential measurement was performed to get the surface charge of the vesicles at different concentrations. The data collected in Table S2 (see SI) show that the  $\zeta$ -potential values are almost zero, which is highly expected as the surfactants are present in the zwitterionic form in pH 7 buffer. As the vesicles are charge-neutral at pH 7, there remains some possibility of vesicle-vesicle interactions which enhances the size of the vesicles, as

indicated by the small change in turbidity of the surfactant solutions when stored for a longer period of time.

**Dye Entrapment and Release Kinetics.** To investigate the drug encapsulation and its release profile, we have chosen two water-soluble dyes, such as methylene blue (MB) and calcein (CAL) as model drugs. The encapsulation of MB and CAL into the aqueous core of the vesicles was performed following a method reported elsewhere.<sup>14,58</sup> The encapsulation was confirmed by the characteristic size exclusion chromatogram. The detailed procedure can be found under “Experimental Methods” included in the SI. The peaks with low absorbance at low elution volume correspond to the vesicle entrapped dye molecule. It has been found that there was a small initial portion containing vesicles entrapping approximately 2.77% of the total dye followed by a large peak which was due to the untrapped dye (see Figure S13 in SI).

Following the same procedure CAL was also entrapped in the vesicles in pH 7.4. The encapsulation was confirmed by the characteristic fluorescence spectra of the dye (see Figure S14 of SI). The release study using entrapped CAL was carried out in pH 3.0 buffer at 37 °C. It can be observed that when an aliquot of dilute HCl solution was added (to attain pH 3.0) to the vesicular solutions containing CAL, the fluorescence intensity of the dye decreased immediately by a large extent. This can be attributed to the burst release ( $\sim 55\%$ ) of the dye molecules due to the large change in permeability of the bilayer membrane as a result of a change in ionization behavior of the amphiphile in acidic pH (see Scheme 1). Another factor which plays an important role is the acid hydrolysis of the ester linkage which causes the release of dye molecules by disrupting the vesicle membrane. Consequently, after the rapid initial decrease the fluorescence intensity of the dye decreased slowly with time. The fluorescence spectra were therefore recorded at different time intervals following the burst release. The % release of dye molecule was calculated from the relative fluorescence intensities at the emission maximum using the equation  $(1 - I/I_0) \times 100\%$ , where  $I$  and  $I_0$  are the fluorescence intensities at any time  $t$  and at the start of the experiment, respectively. From the representative release profile (Figure 8) for mPEG<sub>300</sub>-Cys amphiphile it is obvious that following burst release a slow release occurs, reaching a plateau at about 62%. The slow release can be attributed to the disruption of the vesicle membrane due to acid catalyzed hydrolysis of the ester linkage. The release of the model drug CAL at pH 7.4 was also carried out as a control study. The release profile is included in Figure

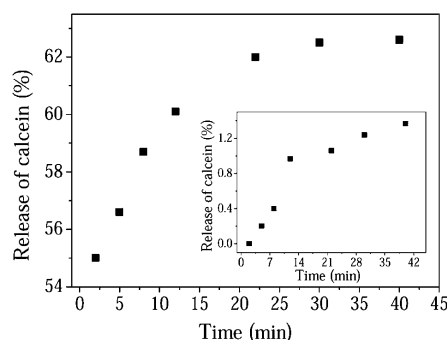


**Figure 8.** Release of calcein (%) with the variation of time (min) of mPEG<sub>300</sub>-Cys at pH 3.0 and 37 °C (inset: calcein release profile at pH 7.4).

8. It can be observed that there is almost zero percent release of the dye within the experimental time period of 2 h.

A similar experiment using the hydrophobic dye DPH was also carried out in both surfactant solutions. The release profiles are shown in SI Figure S15. In this case also, a burst release (35%) followed by a slow release (up to 50%) was observed, and the control experiment at pH 7.4 did not show any release during the period of experiment. The results of these experiments show that the self-assembled vesicular structures of mPEG<sub>300</sub>-Cys and mPEG<sub>1100</sub>-Cys amphiphiles can be used as efficient sustained-release delivery systems in pharmaceutical applications.

## CONCLUSIONS

Two novel L-cysteine-based zwitterionic surfactants with mPEG tail were synthesized and characterized. The surface activity and aggregation behavior were thoroughly examined in pH 7.0 buffer at 25 °C. On the basis of the experimental results of surface tension, fluorescence, DLS, and TEM measurements, the amphiphiles were found to be less surface active, but were observed to have strong tendency to self-organize spontaneously to form stable unilamellar vesicles in dilute as well as in concentrated solutions. Unlike amino acid-based hydrocarbon surfactants, a relatively polar but rigid bilayer membrane is observed to form by the mPEG chains. The thermodynamics of vesicle formation was observed to be very similar to conventional hydrocarbon surfactants. The large positive values of  $\Delta S_m^\circ$  indicate that the driving force behind the spontaneous vesicle formation is hydrophobic interaction. The vesicles were observed to be stable in the temperature range 20–75 °C over a long period of time. The amphiphiles exhibit vesicle formation in both acidic and basic pH. The vesicles were found to be capable of encapsulating hydrophilic as well as hydrophobic dyes. However, the vesicles are sensitive to pH change and therefore can find potential application as efficient sustained drug delivery vehicles in the pharmaceutical industry. Studies on the self-assembly of amphiphilic molecules consisting of mPEG tail and other amino acid head groups are currently underway in this laboratory.

## ASSOCIATED CONTENT

### Supporting Information

Details of synthetic procedure, FT-IR, <sup>1</sup>H NMR, and <sup>13</sup>C NMR spectral data of the synthesized amphiphiles, experimental methods, surface tension plots, representative fluorescence emission spectra of NPN, C153, and Py, size distribution histograms, TEM pictures, gel permeation chromatogram, plots

of turbidity, and kinetic profiles for DPH release. This material is available free of charge via the Internet at <http://pubs.acs.org>.

## AUTHOR INFORMATION

### Corresponding Author

\*Phone: (+) 91-3222-283308. Fax: (+) 91-3222-255303. E-mail: joydey@chem.iitkgp.ernet.in.

### Notes

The authors declare no competing financial interest.

## ACKNOWLEDGMENTS

The authors thank Indian Institute of Technology, Kharagpur for financial support of this work. We are thankful to Prof. N. Sarkar for the DLS and zeta potential measurements.

## REFERENCES

- (1) Kunitake, T.; Mittal, K. L.; Bothorel, P.; Eds. *Surfactants in Solution*; Plenum: New York, 1986; Vol 5, p 727.
- (2) Kissa, E. *Fluorinated Surfactants and Repellents*, 2nd ed.; Marcel Dekker: New York; p 103.
- (3) Fendler, J. H. *Membrane Mimetic Chemistry*; Wiley: New York, 1982; Chapter 6.
- (4) Torchilin, V. P. Recent Advances with Liposomes as Pharmaceutical Carriers. *Nat. Rev. Drug Discovery* **2005**, *4*, 145–160.
- (5) Collier, J. H.; Messersmith, P. B. Phospholipid Strategies in Biomineralization and Biomaterials Research. *Annu. Rev. Mater. Res.* **2001**, *31*, 237–263.
- (6) Lundhal, P.; Yang, Q. Liposome Chromatography: Liposomes Immobilized in Gel Beads as a Stationary Phase for Aqueous Column Chromatography. *J. Chromatogr.* **1991**, *544*, 283–304.
- (7) Chang, H.-I.; Yeh, M.-K. Clinical Development of Liposome-Based Drugs: Formulation, Characterization, and Therapeutic Efficacy. *Int. J. Nanomed.* **2012**, *7*, 49–60.
- (8) Dai, Y.; Zhou, R.; Liu, L.; Lu, Y.; Qi, J.; Wu, W. Liposomes Containing Bile Salts as Novel Ocular Delivery Systems for Tacrolimus (FK506): In Vitro Characterization and Improved Corneal Permeation. *Int. J. Nanomed.* **2013**, *8*, 1921–1933.
- (9) Immordino, M. L.; Dosio, F.; Cattel, L. Stealth Liposomes: Review of the Basic Science, Rationale, and Clinical Applications, Existing and Potential. *Int. J. Nanomed.* **2006**, *1*, 297–315.
- (10) Mimms, L. T.; Zampighi, G.; Nozaki, Y.; Tanford, C.; Reynolds, J. A. Phospholipid Vesicle Formation and Transmembrane Protein Incorporation Using Octyl Glucoside. *Biochemistry* **1981**, *20*, 833–840.
- (11) Yue, B.; Huang, C. H.; Nich, M.-P.; Glinka, C. J.; Katsaras, J. Spontaneously Forming Unilamellar Phospholipid Vesicles. *Macromol. Symp.* **2005**, *219*, 123–133.
- (12) Sumida, Y.; Masuyama, A.; Takasu, M.; Kida, T.; Nakatsuji, Y.; Ikeda, I.; Nojima, M. New pH-Sensitive Vesicles. Release Control of Trapped Materials from the Inner Aqueous Phase of Vesicles Made from Triple-Chain Amphiphiles Bearing Two Carboxylate Groups. *Langmuir* **2001**, *17*, 609–612.
- (13) Lasic, D. D. In *Vesicles*; Rosoff, M., Ed.; Marcel Dekker: New York, 1996; Vol 62, pp 447–476.
- (14) Bhattacharya, S.; Biswas, J. Vesicle and Stable Monolayer Formation from Simple “Click” Chemistry Adducts in Water. *Langmuir* **2011**, *27*, 1581–1591.
- (15) Kunitake, T.; Okahata, Y.; Shimomura, M.; Yasunami, S.; Takarabe, K. Formation of Stable Bilayer Assemblies in Water from Single-Chain Amphiphiles. Relationship between the Amphiphile Structure and the Aggregate Morphology. *J. Am. Chem. Soc.* **1981**, *103*, 5401–5413.
- (16) Ambühl, M.; Bangerter, F.; Luisi, P. L.; Skrabal, P.; Watzke, H. J. Configurational Changes Accompanying Vesiculation of Mixed Single-Chain Amphiphiles. *Langmuir* **1993**, *9*, 36–38.
- (17) Ghosh, S.; Dey, J. Interaction of Sodium N-lauroylsarcosinate with N-alkylpyridinium Chloride Surfactants: Spontaneous Formation

of pH-responsive, Stable Vesicles in Aqueous Mixtures. *J. Colloid Interface Sci.* **2011**, *358*, 208–216.

(18) Israelachvili, J. N. *Intermolecular and Surface Forces*, 2nd ed.; Academic Press: New York, 1992.

(19) Guida, V. Thermodynamics and Kinetics of Vesicles Formation Processes. *Adv. Colloid Interface Sci.* **2010**, *161*, 77–88.

(20) Antonietti, M.; Förster, S. Vesicles and Liposomes: A Self-Assembly Principle Beyond Lipids. *Adv. Mater.* **2003**, *15*, 1323–1333.

(21) Soussan, E.; Cassel, S.; Blanzat, M.; Rico-Lattes, I. Drug Delivery by Soft Matter: Matrix and Vesicular Carriers. *Angew. Chem., Int. Ed.* **2009**, *48*, 274–288.

(22) Medvedeva, A. D.; Maslov, M. A.; Serikov, R. N.; Morozova, N. G.; Serebrennikova, G. A.; Sheglov, D. V.; Latyshev, A. V.; Vlassov, V. V.; Zenkova, M. A. Novel Cholesterol-Based Cationic Lipids for Gene Delivery. *J. Med. Chem.* **2009**, *52*, 6558–6568.

(23) Bajaj, A.; Mishra, S. K.; Kondaiah, P.; Bhattacharya, S. Effect of the Headgroup Variation on the Gene Transfer Properties of Cholesterol Based Cationic Lipids Possessing Ether Linkage. *Biochim. Biophys. Acta* **2008**, *1778*, 1222–1236.

(24) Bajaj, A.; Kondaiah, P.; Bhattacharya, S. Effect of the Nature of the Spacer on Gene Transfer Efficacies of Novel Thiocholesterol Derived Gemini Lipids in Different Cell Lines: A Structure–Activity Investigation. *J. Med. Chem.* **2008**, *51*, 2533–2540.

(25) Bhattacharya, S.; De, S.; George, S. K. Synthesis and Vesicle Formation from Novel Pseudoglycerol Dimeric Lipids. Evidence of Formation of Widely Different Membrane Organizations with Exceptional Thermotropic Properties. *Chem. Commun.* **1997**, 2287–2288.

(26) Smuldes, E. In *Laundry Detergents*; Wiley-VCH Verlag GmbH, 2002; Part 3, pp 38–98.

(27) Dey, J.; Shrivastava, S. Can Molecules with Anionic Head and Poly(ethylene glycol) methyl ether Tail Self-assemble in Water? A Surface tension, Fluorescence probe, Light scattering, and Transmission Electron Microscopic Investigation. *Soft Matter* **2012**, *8*, 1305–1308.

(28) Dey, J.; Shrivastava, S. Physicochemical Characterization and Self-Assembly Studies on Cationic Surfactants bearing mPEG Tail. *Langmuir* **2012**, *28*, 17247–17255.

(29) Tasaki, K. Poly(oxyethylene) Water Interactions: A Molecular Dynamics Study. *J. Am. Chem. Soc.* **1996**, *118*, 8459–8469.

(30) Zaslavsky, B. Y.; Baevskii, A. V.; Rogozhin, S. V.; Gedrovich, A. V.; Shishkov, A. V.; Gasanov, A. A.; Masimov, A. A. Relative Hydrophobicity of Synthetic Macromolecules: I. Polyethylene glycol, Polyacrylamide and Polyvinylpyrrolidone. *J. Chromatogr.* **1984**, *285*, 63–68.

(31) Carstens, M. G.; van Nostrum, C. F.; Ramji, A.; Meeldijk, J. D.; Verrijck, R.; de Leede, L. L.; Crommelin, J. A.; Hennink, W. E. Poly(ethylene glycol)–oligolactates with Monodisperse Hydrophobic blocks: Preparation, Characterization, and Behavior in Water. *Langmuir* **2005**, *21*, 11446–11454.

(32) Park, M. J.; Chung, Y. C.; Chun, C. B. PEG-based Surfactants that Show High Selectivity in Disrupting Vesicular Membrane with or without Cholesterol. *Colloids Surf., B* **2003**, *32*, 11–18.

(33) Katayose, S.; Kataoka, K. Remarkable Increase in Nuclease Resistance of Plasmid DNA through Supramolecular Assembly with Poly(ethylene glycol)–poly(L-lysine) block Copolymer. *J. Pharm. Sci.* **1998**, *87*, 160–163.

(34) Trubetskoy, V. S.; Torchilin, V. P. Use of Polyoxyethylene-lipid Conjugates as Long-circulating Carriers for Delivery of Therapeutic and Diagnostic Agents. *Adv. Drug Delivery Rev.* **1995**, *16*, 311–320.

(35) Morikawa, H.; Koike, S.; Saiki, M.; Saegusa, Y. Synthesis and Characterization of the PEG-based Nonionic Surfactants Endowed with Carboxylic Acid Moiety at the Hydrophobic Terminal. *J. Polym. Sci., Part A: Polym. Chem.* **2008**, *46*, 8206–8212.

(36) Yoshimura, T.; Nyuta, K.; Esumi, K. Zwitterionic Heterogemini Surfactants Containing Ammonium and Carboxylate Headgroups. I. Adsorption and Micellization. *Langmuir* **2005**, *21*, 2682–2688.

(37) Lomax, E. G. In *Amphoteric Surfactants*, 2nd ed.; Surfactant Science Series; Marcel Dekker: New York, 1996; Vol 59, pp 75–190.

(38) Domingo, X. In *Amphoteric Surfactants*; Lomax, E. G., Ed.; Surfactant Science Series; Marcel Dekker: New York, 1996; Vol. 59, Chapter 3.

(39) Mohanty, A.; Dey, J. Spontaneous Formation of Vesicles and Chiral Self-Assemblies of Sodium N-(4-Dodecyloxybenzoyl)-L-Valinate in Water. *Langmuir* **2004**, *20*, 8452–8459.

(40) Patra, T.; Ghosh, S.; Dey, J. Spontaneous Formation of pH-sensitive, Stable Vesicles in Aqueous Solution of N-[4-n-octyloxybenzoyl]-L-histidine. *Soft Matter* **2010**, *6*, 3669–3679.

(41) Ghosh, S.; Das Mahapatra, R.; Dey, J. Thermoreversible as Well as Thermoirreversible Organogel Formation by L-Cysteine-Based Amphiphiles with Poly(ethylene glycol) Tail. *Langmuir* **2014**, *30*, 1677–1685.

(42) Posner, A. M.; Anderson, J.R.; Alexander, A. E. The Surface Tension and Surface Potential of Aqueous Solutions of Normal Aliphatic Alcohols. *J. Colloid Sci.* **1952**, *7*, 623–644.

(43) Ananthapadmanabhan, K. P.; Goddard, E. D.; Turro, N. J.; Kuo, P. L. Fluorescence Probes for Critical Micelle Concentration. *Langmuir* **1985**, *1*, 352–355.

(44) Saitoh, T.; Taguchi, K.; Hiraide, M. Evaluation of Hydrophobic Properties of Sodium Dodecylsulfate/ $\gamma$ -Alumina Admicelles Based on Fluorescence Spectra of N-Phenyl-1-Naphthylamine. *Anal. Chim. Acta* **2002**, *454*, 203–208.

(45) Chapman, C. F.; Fee, R. S.; Maroncelli, M. Measurements of the Solute Dependence of Solvation Dynamics in 1-Propanol: The Role of Specific Hydrogen-Bonding Interactions. *J. Phys. Chem.* **1995**, *99*, 4811–4819.

(46) Horng, M. L.; Gardecki, J. A.; Papazyan, A.; Maroncelli, M. Subpicosecond Measurements of Polar Solvation Dynamics: Coumarin 153 Revisited. *J. Phys. Chem.* **1995**, *99*, 17311–17337.

(47) Kalyanasundaram, K.; Thomas, J. K. Environmental Effects on Vibronic Band Intensities in Pyrene Monomer Fluorescence and Their Application in Studies of Micellar Systems. *J. Am. Chem. Soc.* **1977**, *99*, 2039–2044.

(48) Kalyanasundaram, K. *Photophysics of Microheterogeneous Systems*; Academic Press: New York, 1988.

(49) Shinitzky, M.; Barenholz, Y. Dynamics of the Hydrocarbon Layer in Liposomes of Lecithin and Sphingomyelin Containing Dicylphosphate. *J. Biol. Chem.* **1974**, *249*, 2652–2657.

(50) Roy, S.; Mohanty, A.; Dey, J. Microviscosity of Bilayer membranes of some N-Acylamino Acid Surfactants determined by Fluorescence Probe Method. *Chem. Phys. Lett.* **2005**, *414*, 23–27.

(51) Lakowicz, J. R. *Principles of Fluorescence Spectroscopy*; Plenum Press: New York, 1983; p 132.

(52) Cehelnik, E. D.; Cundall, R. B.; Lockwood, J. R.; Palmer, T. F. Solvent and Temperature Effects on the Fluorescence of all-trans-1,6-diphenyl-1,3,5-hexatriene. *J. Phys. Chem.* **1975**, *79*, 1369–1376.

(53) Clint, J. H. *Surfactant Aggregation*; Chapman and Hall: New York, 1991.

(54) Paula, S.; Siis, W.; Tuchtenhagen, J.; Blume, A. Thermodynamics of Micelle Formation as a Function of Temperature: A High Sensitivity Titration Calorimetry Study. *J. Phys. Chem.* **1995**, *99*, 11742–11751.

(55) Verral, R. E.; Milioto, S.; Zana, R. Ternary Water-in-oil Microemulsions Consisting of Cationic Surfactants and Aromatic Solvents. *J. Phys. Chem.* **1988**, *92*, 3939–3943.

(56) Majhi, P.; Moulik, S. Energetics of Micellization: Reassessment by a High-Sensitivity Titration Microcalorimeter. *Langmuir* **1998**, *14*, 3986–3990.

(57) Jusufi, A.; Antti-Pekka Hynninen, A. P.; Haataja, M.; Panagiotopoulos, A. Z. Electrostatic Screening and Charge Correlation Effects in Micellization of Ionic Surfactants. *J. Phys. Chem. B* **2009**, *113*, 6314–6320.

(58) Bhattacharya, S.; Ghanashyam Acharya, N. S. Vesicle and Tubular Microstructure Formation from Synthetic Sugar-linked Amphiphiles. Evidence of Vesicle Formation from Single-chain Amphiphiles Bearing a Disaccharide Headgroup. *Langmuir* **2000**, *16*, 87–97.